ISSN 1560-3547, Regular and Chaotic Dynamics, 2016, Vol. 21, Nos. 7–8, pp. 939–954. © Pleiades Publishing, Ltd., 2016.

Spiral Chaos in the Nonholonomic Model of a Chaplygin Top

Alexey V. Borisov[1*], Alexey O. Kazakov[2], and Igor R. Sataev[1,3***]**

[1] *Udmurt State University,*
ul. Universitetskaya 1, Izhevsk, 426034 Russia

[2] *National Research University Higher School of Economics,*
ul. Bolshaya Pecherskaya 25/12, Nizhny Novgorod, 603155 Russia

[3] *Institute of Radio Engineering and Electronics RAS, Saratov Branch*
ul. Zelenaya 38, Saratov, 410019 Russia

Received October 12, 2016; accepted November 29, 2016

Abstract—This paper presents a numerical study of the chaotic dynamics of a dynamically asymmetric unbalanced ball (Chaplygin top) rolling on a plane. It is well known that the dynamics of such a system reduces to the investigation of a three-dimensional map, which in the general case has no smooth invariant measure. It is shown that homoclinic strange attractors of discrete spiral type (discrete Shilnikov type attractors) arise in this model for certain parameters. From the viewpoint of physical motions, the trace of the contact point of a Chaplygin top on a plane is studied for the case where the phase trajectory sweeps out a discrete spiral attractor. Using the analysis of the trajectory of this trace, a conclusion is drawn about the influence of "strangeness" of the attractor on the motion pattern of the top.

MSC2010 numbers: 37J60, 37N15, 37G35, 70E18, 70F25, 70H45

DOI: 10.1134/S1560354716070157

Keywords: nonholonomic constraint, spiral chaos, discrete spiral attractor

INTRODUCTION

1. This paper is concerned with a dynamical system describing the rolling motion of a heavy ball on a plane for which all central moments of inertia are different and the center of mass does not lie in any of the principal planes of inertia. Following [1, 2], we shall call this system a *Chaplygin top*. It is assumed that the velocity of the contact point is zero, which leads to nonintegrable constraints. Problems of this kind are treated in nonholonomic mechanics (for its development, see the recent review [3]).

In the case where the center of mass of the ball coincides with its geometric center, we obtain the classical Chaplygin ball rolling problem [4] (1903), in which the equations of motion are integrable by quadratures. Consequently, the Chaplygin ball exhibits regular behavior. A qualitative analysis of this behavior is presented in [5].

As compared to the Chaplygin ball, the dynamics of the Chaplygin top is much more complex. In this case, the system is characterized by chaotic motions and can have, depending on the system parameters, simple or strange attractors [2, 6]. The existence of strange attractors for nonholonomic systems was originally reported in [7–9] (where a rattleback is considered as an example) and is closely related to the absence (in the general case for nonholonomic systems) of an invariant measure with smooth density [10].

2. The system dealt with in this paper possesses an energy integral, i.e., it is conservative. This is due to the fact that in the case of ideal rolling the reaction forces of constraints do not do any

*E-mail: borisov@rcd.ru
**E-mail: kazakovdz@ya.ru
***E-mail: sataevir@rambler.ru

work, and the attractors themselves arise on the level surface of this integral. The conditions for the existence of an energy integral for nonholonomic systems have been discussed recently in [11, 12].

The study of the dynamics of a Chaplygin top is a particular case of the general description of the rolling motion of rigid bodies on a plane $\mathbf{R}^2$ and a sphere $\mathbf{S}^2$, which is systematically treated in [13]. The existence of various tensor invariants (first integrals, symmetry fields, Poisson structure and invariant measure) depending on the geometrical and dynamical parameters of the rolling body is analyzed in [13]. This concept, which was called the *hierarchy of dynamics* of nonholonomic systems, points to the fact that they differ from Hamiltonian systems. Moreover, it was noted in [13] that in the case of a rigid body rolling without slipping on $\mathbf{R}^2$ and $\mathbf{S}^2$ the analysis of dynamics generally reduces to analysis of a three-dimensional Poincaré map.

The three-dimensional point map, which arises in other problems, was analyzed by numerical and analytical methods in [14–17] in relation to the Lorenz and Rössler models. We note that the concept of hyperchaos proposed by Rössler in 1979 [18, 19] was motivated by the study of four-dimensional flows, which obviously reduce to three-dimensional maps. In addition, in [19] the first example was given of a formal three-dimensional map that admits a strange hyperchaotic attractor. Formal three-dimensional dissipative Hénon maps were studied in [14, 20] from the viewpoint of the existence of various strange attractors and quasi-periodic bifurcations, respectively.

As an interesting remark, we note that nowadays three-dimensional volume-preserving point maps [21, 22] are of the greatest interest to researchers. Examples of such maps relevant to nonholonomic mechanics were first given for systems describing the dynamics of a ball rolling on various surfaces [23, 24].

3. Since there is no invariant measure in the system discussed in this paper (and in [7, 13]), it may be classified as dissipative. However, as opposed to the real mechanical dissipation, the dissipation that arises formally due to nonholonomic constraints is rather specific ("nonholonomic") in nature. *Nonholonomic dissipation* is still poorly understood, but its typical feature is that regions of expansion and contraction of the phase volume (arising due to sign-alternating divergence) coexist in phase space. In addition, systems of this kind admit, generally speaking, several involutions such as those analyzed in [25]. The equations of motion for a Chaplygin top possess only one involution, since its center of mass does not lie in any of the principal planes of inertia. Nevertheless, even in this case to each attractor in phase space there corresponds a repeller symmetric to it, and this reversibility is also essential for analysis of bifurcations. We also note that, in view of the specific properties of nonholonomic dissipation, nonholonomic systems are sometimes said to occupy an intermediate position between dissipative and Hamiltonian systems (see, e.g., [26]).

Due to the specificity of nonholonomic dissipation, the appearance of various strange attractors (as predicted by general theory) in particular nonholonomic systems is somewhat unusual, especially as each of them is associated with a specific type of dynamical behavior. We note that, for many nonholonomic systems without an invariant measure with smooth density, strange attractors usually coexist with another dynamical phenomenon, that of reversal. It was in rattleback dynamics that the reversal was experimentally observed for the first time (see, e.g., [7]). Later, the reversal was theoretically predicted for the Chaplygin top [2] and for the Suslov problem [27].

4. Previously, a figure-eight attractor was found for the Chaplygin top (see [2]). By this we mean discrete attractors that, in contrast to flow attractors, are defined for three-dimensional maps. The figure-eight attractor, like the discrete Lorenz attractor pointed out in rattleback dynamics [9], is homoclinic, that is, it arises from a hyperbolic point (for which an intersection of the stable and the unstable manifold belongs to the attractor. In [28], a scenario was described for the appearance of a *discrete spiral attractor* (or Rössler or Shilnikov attractor), which was numerically found for the model Hénon map [20]. General concepts and applications of spiral attractors, which arise both in flows and in maps, are presented in Section 1 of this paper.

In this paper, by constructing charts of Lyapunov exponents on the plane of system parameters and by analyzing local and global bifurcations, we point out and study two types of discrete spiral attractors in the system under consideration: homoclinic attractors (on the basis of the homoclinic structure of a saddle-focus point) and heteroclinic attractors (on the basis of the heteroclinic structure of a saddle-focus point of period 2.

5. In the conclusion, we consider the motion of the contact point of the ball in the case where the phase trajectory sweeps out a spiral attractor. In contrast to the generally accepted notion

of a chaotic (or even hyperchaotic) spiral attractor, it makes no significant contribution to the conditionally periodic dynamics of the contact point. As shown in [29], for the trajectory of the contact point to be strongly chaotic, the attractor must occupy a much larger region in phase space. It turns out that in this case, in addition to chaotic diffusion, directed drift is possible, which is pointed out for nonautonomous nonholonomic systems in [30]. In this paper, we consider the trajectory of the contact point very briefly, but it should be stressed that its analysis is a very important dynamical problem (treated for the Chaplygin ball in [5]).

Indeed, it would be interesting to experimentally discover the effects of dynamical behavior described in this paper and in [2, 9], since the trace of the contact point on the plane lends itself to simple measurement. We note that the study of the behavior of dynamically asymmetric balls has been motivated recently by problems of mobile robotics which are related to the design of a controlled spherical robot (sphericle); for a review of relevant literature see [31–33]. The chaoticity of the trajectory of the contact point can be regarded as a factor that not only prevents control, but also makes it sometimes possible to use it for producing a directed drift [34] (see also [29, 30]). The fairly regular behavior of the contact point on the strange attractor agrees with a similar behavior of the contact point on the discrete Lorenz attractor, which is discussed in [35].

In the case of displacement of the center of mass, but in the absence of a gravitational field, as shown in [13], there exists an additional first integral quadratic in the angular velocities. On the level surface of this integral in the Poincaré section there are, as a rule, only simple attractors which define quasi-periodic double-frequency motions in absolute space.

6. In the future, it would be interesting to explore the dynamics of a Chaplygin top on a sphere [13]. The system is chaotic even if the center of mass coincides with the geometric center, but possesses an invariant measure. Of particular interest is the case of behavior of such a system in the absence of a gravitational field, which also reduces to a three-dimensional map. An interesting integrable case which generalizes the classical system of a Chaplygin ball rolling on a plane and takes place at a certain ratio between the radii of the fixed sphere and the rolling ball was found and analyzed in [36–38].

1. SPIRAL VS DISCRETE SPIRAL CHAOS

We give a brief review of research on spiral chaos in three-dimensional flows. These studies go back to the work of L. P. Shilnikov (1965) [39]. The theorem proved by L. P. Shilnikov states that near a separatrix loop of a saddle-focus equilibrium (see Fig. 1a), subject to some additional conditions imposed on the eigenvalues of this equilibrium state, there exists a countable set of periodic saddle trajectories, resulting in complex behavior of the system near the loop. In fact, the theorem gives a simple criterion for the existence of chaos for a wide class of systems possessing a separatrix loop of a saddle-focus. Afterwards, this kind of chaos was called *spiral chaos*[1)] or *Shilnikov's chaos*.

However, we note that, subject to the conditions of Shilnikov's theorem, the appearance of complex dynamics related to the existence of a countable set of periodic saddle trajectories does not always lead to the appearance of strange attractors. Moreover, complex dynamics may not manifest itself at all. For example, if the system is given on a noncompact manifold, the trajectories started in a neighborhood of a loop of a saddle-focus can escape to infinity. Also, the trajectories can escape to simple (regular) attractors, whose emergence are not connected with a loop. An additional necessary condition for a strange attractor to arise from a loop of a saddle-focus is the existence of an absorbing region that must not have any simple (regular) attractors. The strange attractor arising in this case is called a *spiral attractor* (other names are the Shilnikov attractor or the Rössler attractor).

As an example, Fig. 1b shows a phase portrait of a spiral attractor for the Rössler system [40, 41] with the parameter values a = 0.43, b = 0.4, c = 4.5. The spectrum of Lyapunov exponents in this case is $(\Lambda_1 \approx 0.119, \Lambda_2 \approx 0.0, \Lambda_3 \approx -3.75)$, and the dimension according to Kaplan – Yorke is $D \approx 2 + 0.119/3.75 \approx 2.03$.

[1)] Note that the term *spiral chaos* was first introduced in 1976 by O. E. Rössler [40]. Apparently the author did not know of the work of Shilnikov and called the chaos arising in his model *spiral chaos* (see Fig. 1b). It was shown in [41] that spiral chaos discovered in [40] arises near a separatrix loop of a saddle-focus.

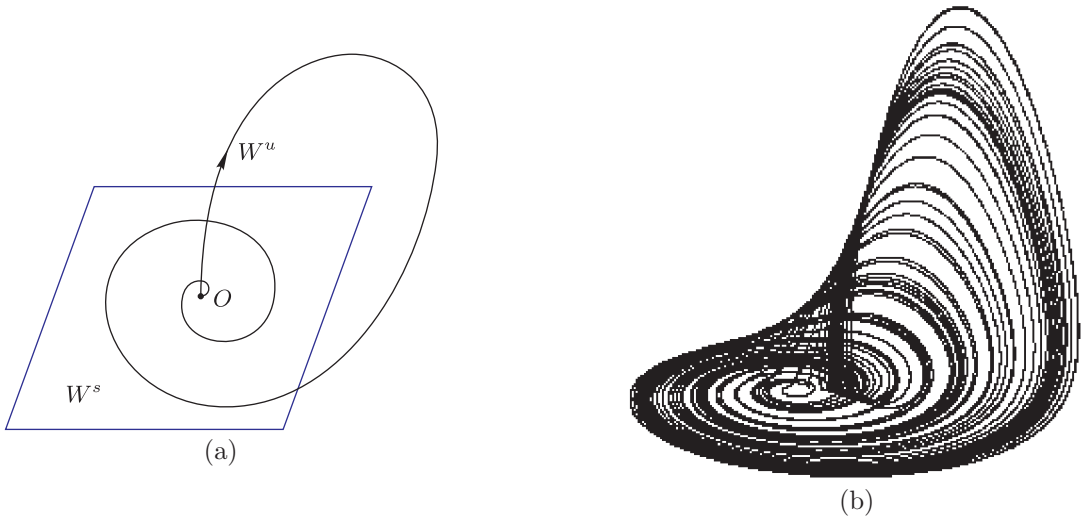

Fig. 1. (a) Separatrix loop of a saddle-focus with a two-dimensional stable manifold and a one-dimensional unstable manifold, (b) Spiral attractor in the Rössler system [40, 41].

The papers [41–43] were the first to show numerically the appearance of a spiral attractor. In all probability, it was these papers that drew the attention of Western scientists to the discovery of spiral chaos. They were followed by a large number of studies on specific systems from very different applications, in which the authors used different methods to establish the existence of a loop of a saddle-focus and thus proved that the discovered strange attractors are of spiral type. Thus, the authors succeeded in finding spiral attractors in phase synchronization systems [44], radioelectronic devices, such as the Chua contour [45] and the Anishchenko – Astakhov radio generator [46], optical laser systems [47–50], chemical reactions [51, 52], glow discharge systems [53], in some class of models describing the behavior of neurons [54], biophysical experiments [55], electromechanical systems [56, 57], electrochemical processes [58, 59], nonlinear convection in magnetic fields [60], mechanical systems [61] etc.

Chaos of spiral type, like other kinds of chaotic behavior typical of three-dimensional systems, such as the Hénon attractor or the Lorenz attractor, can also be observed in systems of greater dimension. However, systems with dimension $n \geqslant 4$ can exhibit new types of chaotic behavior which are impossible in a system with smaller dimension. Discrete spiral chaos is an example of such behavior. Discrete spiral chaos is associated with the appearance of a homoclinic intersection of a stable and an unstable manifold of the saddle-focus limit cycle (a fixed saddle-focus point in the case of transition to a map, see Fig. 2a).

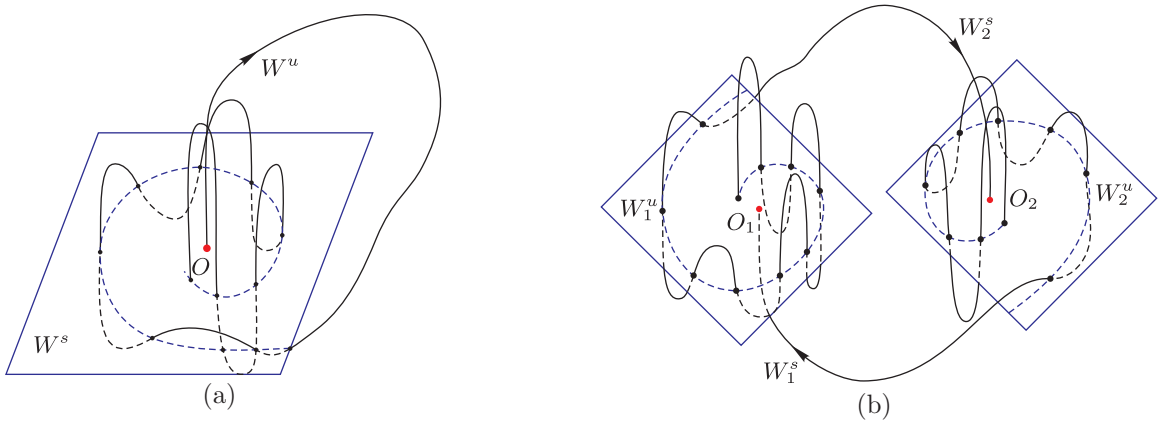

Fig. 2. Homoclinic (a) and heteroclinic (b) structures for three-dimensional maps

Since this has to do with homoclinic Poincaré trajectories to the hyperbolic fixed point of a three-dimensional map (corresponding to a periodic solution of the flow), we point out two essential differences from the homoclinics to an equilibrium for three-dimensional flows:

- the existence of a homoclinic Poincaré trajectory (in the general case) entails the appearance of a Smale horseshoe [62, 63] and hence complex dynamics.
- the homoclinic Poincaré trajectory corresponds to the intersection of manifolds (which is impossible for equilibrium states) and is generally rough, that is, it exists on some interval of parameter values.

Thus, in a neighborhood of a rough homoclinic Poincaré trajectory of a hyperbolic fixed point, complex dynamics arises always, and its type is determined by the type of this hyperbolic point. In the case of a fixed saddle point a discrete Lorenz attractor or a figure-eight attractor can arise, and in the case of a saddle-focus point there appears a discrete spiral attractor [20, 28].

It should be noted that in some systems one can observe another homoclinic situation related to the emergence of a heteroclinic structure on the basis of two saddle-focus points or on the basis of a saddle-focus point of period 2 (see Fig. 2b). It should also be noted that in the case of spiral chaos for three-dimensional flows one distinguishes two types of attractors: spiral attractors and screw attractors [64–66]. To date no such classification has been made for discrete spiral chaos.

A possible scenario of the emergence of a discrete attractor was presented in [28], and in [20] such an attractor was found in a model three-dimensional map. The possibility of appearance of a discrete spiral attractor was discussed in [67].

In what follows, by constructing and analyzing the charts of Lyapunov exponents, we show that discrete spiral attractors can be observed in the nonholonomic model of a Chaplygin top. In addition, in Section 4 we give a detailed description of bifurcations leading to the emergence of spiral attractors from regular regimes and of the properties of the discovered spiral attractors.

2. EQUATIONS OF MOTION OF A CHAPLYGIN TOP

Consider the motion of a dynamically asymmetric ball located in a gravitational field and rolling on a horizontal plane without slipping. The center of mass of the ball is displaced relative to the geometric center by the vector $\boldsymbol{a} = (a_1, a_2, a_3)$. Here and below, we assume that all vectors are given in a coordinate system $Cxyz$ located at the center of mass of the ball and directed along the principal axes of inertia. Let $\mathbf{r}$ denote the radius vector from the the center of mass of the ball to the contact point, and let $\mathbf{v}$ and $\boldsymbol{\omega}$ denote the velocity of the center of mass and the angular velocity of the ball, respectively. Then the no-slip condition (nonholonomic constraint) can be represented as

$$\mathbf{v} + \boldsymbol{\omega} \times \mathbf{r} = 0,$$

and the equations of motion for the angular momentum $\mathbf{M}$ relative to the contact point and the unit normal vector $\boldsymbol{\gamma}$ take the form (see, e.g., [68])

$$\begin{aligned} \dot{\mathbf{M}} &= \mathbf{M} \times \boldsymbol{\omega} + m\dot{\mathbf{r}} \times (\boldsymbol{\omega} \times \mathbf{r}) + m\mathrm{g}_0 \mathbf{r} \times \boldsymbol{\gamma}, \\ \dot{\boldsymbol{\gamma}} &= \boldsymbol{\gamma} \times \boldsymbol{\omega}, \end{aligned} \tag{2.1}$$

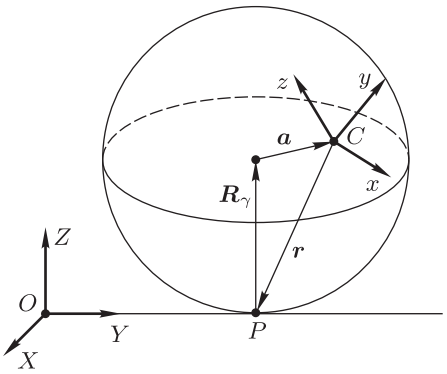

Fig. 3. The Chaplygin top on a plane. $OXYZ$ is a fixed coordinate system, $Cxyz$ is a coordinate system attached to the center of mass of the ball, in which the tensor of inertia of the ball is diagonal, i.e., $\mathbf{I} = \mathrm{diag}(I_1, I_2, I_3)$.

where m is the mass of the ball and g_0 is the free-fall acceleration. The vector $\boldsymbol{\omega}$ is expressed in terms of $\mathbf{M}$ (see, e.g., [23]) by the relation

$$\mathbf{M} = \mathbf{I}\boldsymbol{\omega} + m\mathbf{r} \times (\boldsymbol{\omega} \times \mathbf{r}),$$

where $\mathbf{I} = \mathrm{diag}(I_1, I_2, I_3)$ is the tensor of inertia of the top with principal moments of inertia I_1, I_2 and I_3, and the vectors $\boldsymbol{\gamma}$ and $\mathbf{r}$ for the ball of radius R are related by

$$\mathbf{r} = -R\boldsymbol{\gamma} - \boldsymbol{a}.$$

To recover the motion of the Chaplygin top in absolute space, we need to supplement the system (2.1) with equations describing the position of the center of mass of the ball (X_C, Y_C) in the plane (OXY) and with equations for the orthogonal pair of unit vectors $(\boldsymbol{\alpha}, \boldsymbol{\beta})$ lying in the plane (OXY) and defining (together with the vector $\boldsymbol{\gamma}$) the orientation of the body in absolute space [25].

$$\begin{gathered} \dot{X_C} = R(\boldsymbol{\beta}, \boldsymbol{\omega}), \quad \dot{Y_C} = -R(\boldsymbol{\alpha}, \boldsymbol{\omega}), \\ \dot{\boldsymbol{\alpha}} = \boldsymbol{\alpha} \times \boldsymbol{\omega}, \quad \dot{\boldsymbol{\beta}} = \boldsymbol{\beta} \times \boldsymbol{\omega}. \end{gathered} \tag{2.2}$$

Relations (2.1) define a closed system of equations relative to the vectors $\mathbf{M}$ and $\boldsymbol{\gamma}$. In the case of an arbitrary parameter $\boldsymbol{a}$, this system possesses only two integrals, the geometric integral and the energy integral:

$$\boldsymbol{\gamma}^2 = 1, \quad E = \frac{1}{2}\,\mathbf{M} \cdot \boldsymbol{\omega} - m\mathrm{g}_0 \mathbf{r} \cdot \boldsymbol{\gamma},$$

and hence, the Euler – Jacobi integrability requires finding two additional first integrals and an invariant measure.

In the six-dimensional phase space on the manifold given by the condition of constancy of two integrals of motion, equations (2.1) define a four-dimensional flow. The value of the energy integral E in this case can be regarded as another parameter of the system.

3. TRANSITION TO CHAOS VIA A SEQUENCE OF TORUS DOUBLING BIFURCATIONS

A detailed analysis of the transition from order to chaos in the nonholonomic model of a Chaplygin top using charts of Lyapunov exponents is presented in [2, 6]. Figure 4 presents the fragment of interest on the chart of Lyapunov exponents on the parameter plane (E, a_3); the other parameters are fixed by the following values:

$$I_1 = 2, \quad I_2 = 6, \quad I_3 = 7, \quad a_1 = 1, \quad a_2 = 1.5, \quad \mathrm{g}_0 = 100, \quad R = 3, \quad m = 1. \tag{3.1}$$

The wide strip denoted on the chart by the symbol Q corresponds to the region of stability of the 2-round torus T^2. In the Poincaré map $\boldsymbol{F}$ with a secant given by the condition $\gamma_1 M_2 - \gamma_2 M_1 = 0$, to such a torus there corresponds an attractor consisting of two closed invariant curves, which in turn are visited by the orbit of the Poincaré map. In what follows, for illustrative purposes, we shall present fragments of Poincaré maps only in a neighborhood of one of two components of the invariant curve T^2 (see, e.g., Fig. 4a).

We note that each of the components of the invariant curve T^2 contains two components of the cycle of period 4, each of which for the fourfold iterated map $\boldsymbol{F}^{\mathbf{4}}$ is a fixed point of saddle-focus type (1,2); the stable manifold of this point is one-dimensional and the unstable one is two-dimensional. We denote this saddle-focus cycle (the point of period 4 for $\boldsymbol{F}$) by 4SF and two its components lying inside the invariant curve of the fragment of the map by P and C. In accordance with the scenario described in [20, 28], when the invariant curve T^2 breaks down and the one-dimensional stable manifold intersects with the two-dimensional unstable manifold, a discrete spiral attractor can arise, emanating from point 4SF.

Next, we fix the parameter $a_3 = 0.655$ and carry out a one-parameter analysis of the system from point A along the route AB on the chart of Lyapunov exponents, Fig. 4. As the value of the energy parameter E increases, the invariant curve T^2 undergoes a cascade of torus doubling bifurcations (invariant curves, in terms of the Poincaré map). Figures 4b and 4c show the phase portraits of the attractor in the Poincaré map after the first and the second doubling, respectively. Nowadays, in contrast to the cascade of period-doubling bifurcations of fixed points, the cascade of torus doubling bifurcations is considered to be finite, that is, chaos arises after a finite number

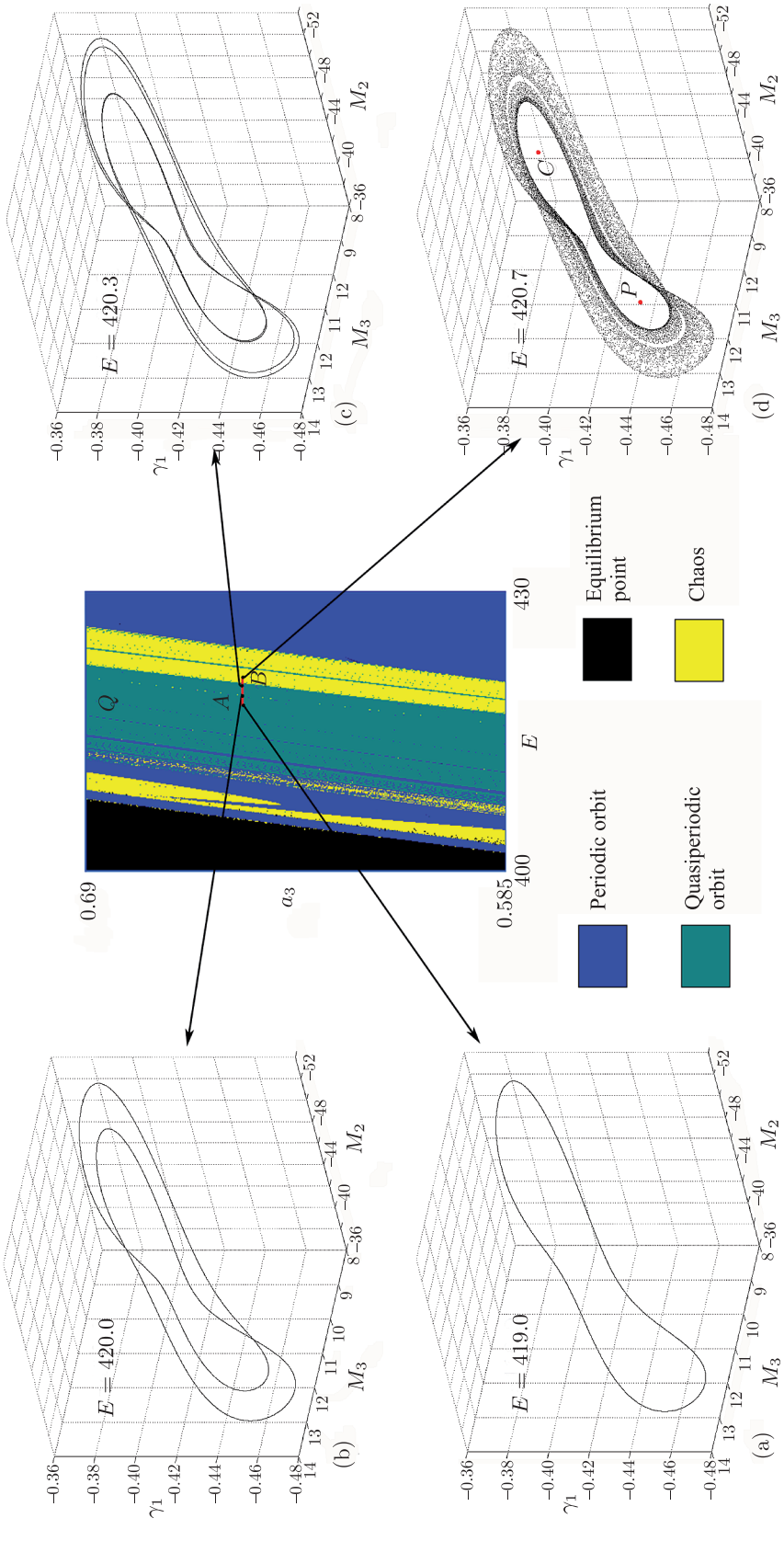

Fig. 4. Chart of Lyapunov exponents for the system (2.1) with parameters (3.1) and typical portraits of the Poincaré map on the secant $\gamma_1 M_2 - \gamma_2 M_1 = 0$ for $a_3 = 0.655$.

of torus doubling bifurcations [69, 70]. This cascade of period doubling bifurcations ends with the emergence of an attractor of torus-chaos type [71, 72], see Fig. 4d.

We note that the attractor shown in Fig. 4d also contains 2 components (P and C) of the periodic saddle-focus point 4SF. It is easy to see that the trajectories of the attractor do not visit the neighborhood of points P and C.

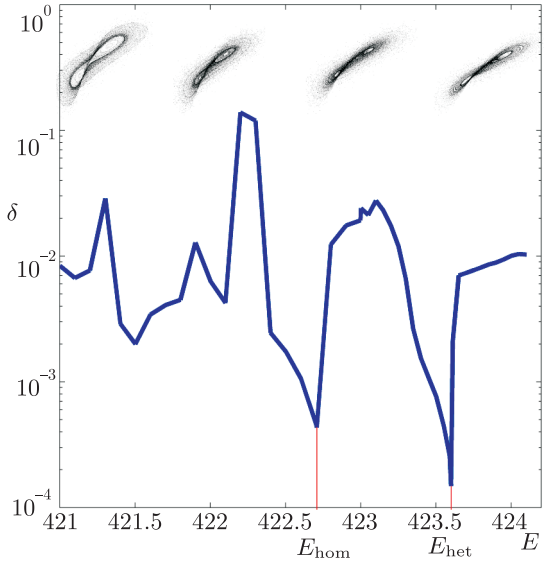

Fig. 5. Graph showing the minimal distance δ from the points of the attractor to one of the components of the saddle-focus depending on E. Typical portraits of the attractor for a Poincaré map with the secant $\gamma_1 M_2 - \gamma_2 M_1 = 0$ at $E \in \{421, 422, 423, 424\}$ are presented above.

As the parameter E is further increased, the attractor gradually begins to occupy the entire internal region, which contains components of the cycle 4SF (see Fig. 5 above). The two-dimensional unstable manifold of the cycle approaches the one-dimensional stable manifold. Such a proximity can be estimated indirectly by constructing a graph of minimal distance δ from the points of the trajectory on the attractor to one of the components of the saddle-focus cycle 4SF depending on the energy parameter E. In the case where the manifolds begin to intersect (when the saddle-focus acquires a homoclinic structure), such a distance tends to zero with increasing number of iterations. The graph described above is shown in Fig. 5. A million iterations of the Poincaré map were performed to obtain one point on the graph. Typical portraits of the attractors for $E \in \{421, 422, 423, 424\}$ are presented in the upper part of the figure. From the graph, one can see 2 pronounced minima corresponding to two different homoclinic situations. We consider each of them separately.

4. DISCRETE SPIRAL CHAOS

4.1. A Homoclinic Discrete Spiral Attractor

As noted above, the region occupied by the torus chaotic attractor contains two fixed points, P and C (see Fig. 4d), of the fourfold iterated Poincaré map $\boldsymbol{F^4}$, each of which possesses a two-dimensional unstable manifold and a one-dimensional stable manifold. It turns out that in such a configuration the presence of a neighboring fixed point is crucial in ensuring that the trajectories of the map return into the neighborhood of the initial fixed point, giving rise to a homoclinic structure of the saddle-focus (1,2). Numerical experiments show that, in the area of the first minimum of the graph shown in Fig. 5, at $E =\approx 422.7$, the stable invariant manifold emanating from point P (in backward time) returns to point P after passing around point C along its unstable manifold. Further behavior greatly depends on the value of the energy parameter. For example, when $E = 422.69$, the stable manifold passes by point P on one side of its unstable manifold, while when $E = 422.71$, it passes by point P on the other side. Thus, somewhere in this range

the manifolds intersect, which implies the emergence of a homoclinic structure like that shown in Fig. 2a. Using the bisection method, we have been able to localize the region of explicit existence of the homoclinic situation to $E \in [422.70065, 422.70070]$. The presence of homoclinics was detected by two visual signs:

- Approach of the stable invariant manifold to a fixed point along the two-dimensional unstable manifold on a spiral trajectory, as shown in Fig. 2a;
- Appearance of typical increasing transverse oscillations as the fixed point itself is approached, which is indicative of a transversal intersection of the manifolds (see again Fig. 2a).

Figure 6 shows invariant manifolds of the fixed point P for the fourfold iterated map $\boldsymbol{F^4}$. When these manifolds intersect, a typical homoclinic structure arises for $E = E_{hom} = 422.70068$.

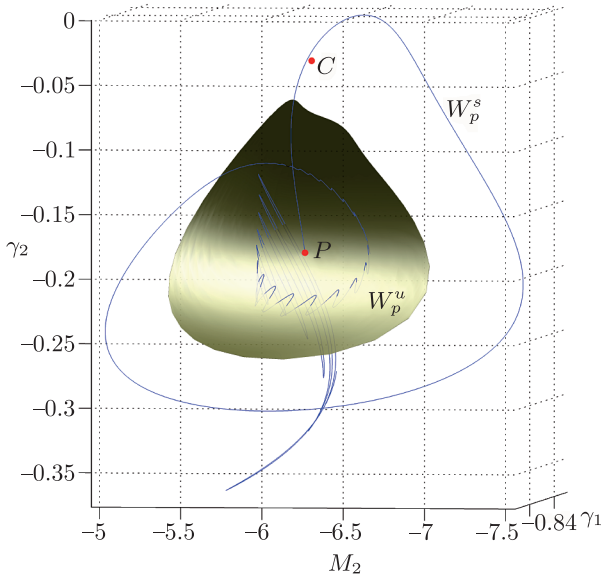

Fig. 6. Intersection of the stable and the unstable manifold of point P (which is fixed for $\boldsymbol{F^4}$).

Remark. One-dimensional invariant manifolds were calculated using an algorithm proposed in [73]. The part of the two-dimensional unstable manifold that immediately adjoins the fixed point was calculated as follows. On a small circle with its center at P, the plane of which coincides with the plane given by two eigenvectors corresponding to complex eigenvalues, a grid was given whose points were iterated several hundreds of times. The resulting grid of points was used to construct an unstable invariant manifold.

Exactly the same homoclinic structure exists in a neighborhood of point C, but the homoclinics of point C are mapped to the homoclinics of point P within two iterations of the Poincaré map (we recall that the phase portraits show only one half of the attractor of period 2). This means that the homoclinic attractor has period 4 (that is, it consists of four subsets which map into each other in turn). Figure 7a shows a phase portrait of the attractor, and Figure 7b presents the same attractor, but shows only each fourth iteration, which corresponds to the attractor in the map $\boldsymbol{F^4}$. It can be seen that only one of the fixed points belongs to such an attractor; the neighborhood of the other point is empty.

It should be noted that in a neighborhood of the above-mentioned homoclinic structure in the parameter E there exists many other homoclinic situations which apparently differ by the number of rotations executed by the stable invariant manifold around the fixed points P and C until it intersects with the unstable manifold. Note also that the attractor arising from each such structure is a discrete spiral attractor.

The spectrum of Lyapunov exponents for the homoclinic discrete spiral attractor is ($\Lambda_1 = 0.0218, \Lambda_2 = 0.0000, \Lambda_3 = -0.113$). The estimate of the correlation dimension of the attractor in the Poincaré section $D_{cor} = 2.12 \pm 0.03$ agrees fairly well with the estimate of the Lyapunov dimension made by the Kaplan – Yorke formula: $D_{K-Y} = 2 + \Lambda_1/|\Lambda_3| \approx 2.19$.

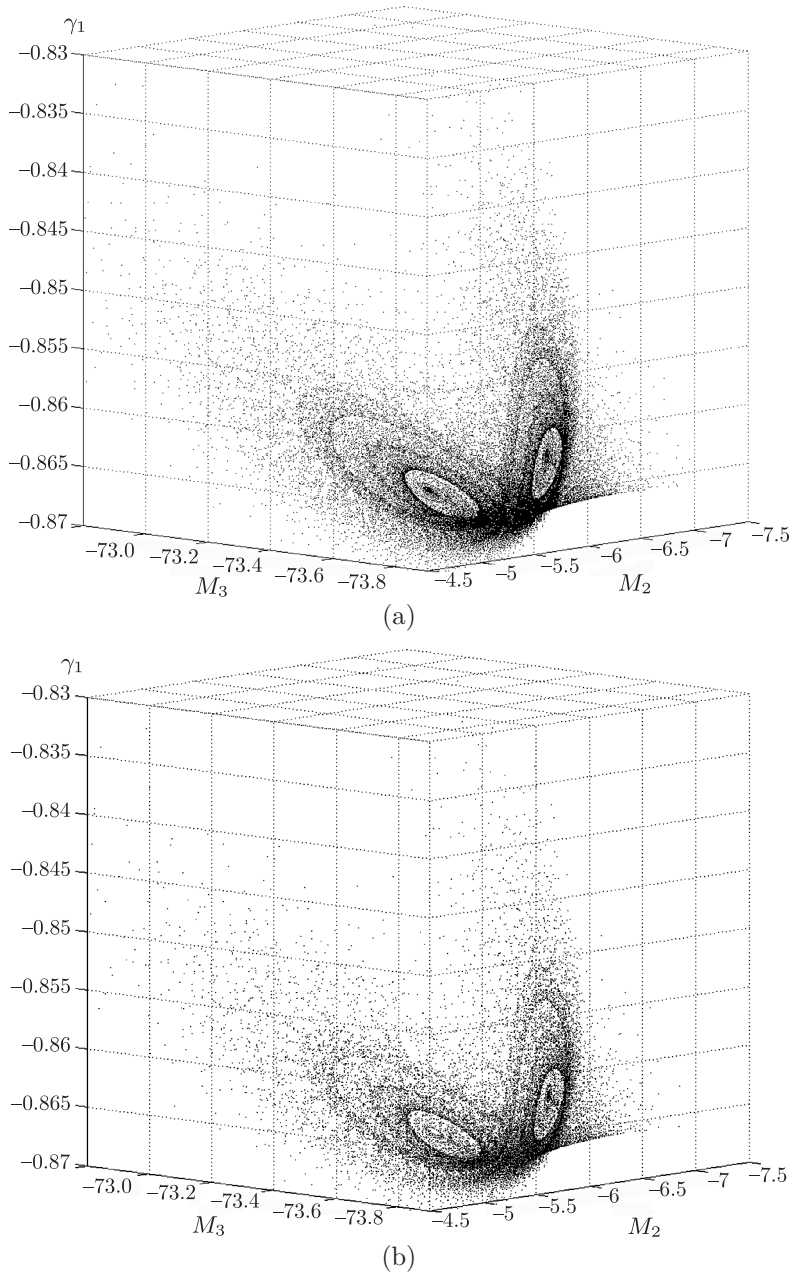

Fig. 7. Phase portraits of a homoclinic discrete spiral attractor for $E = E_{hom} = 422.70068$ on the Poincaré map with the secant $M_1 = 0$: (a) portrait showing each iteration of the map (b) portrait showing each fourth iteration.

4.2. A Heteroclinic Discrete Spiral Attractor

A different homoclinic situation arises for values of the parameter E that correspond to the right minimum in Fig. 5, which is much more pronounced than the left one. The results of numerical experiments show that when $E = E_{het} = 423.59597843$, the one-dimensional stable manifold of the fixed point C of the map $\boldsymbol{F^4}$ enters the neighborhood of the fixed point P and is visually superimposed onto the two-dimensional unstable manifold of this point (see Fig. 8), forming a heteroclinic contour connecting two fixed points of saddle-focus type (1,2) for the map $\boldsymbol{F^4}$.

It should be noted that the homoclinic structure in the case at hand arises from points P and C, which belong to the same limit cycle of system (2.1), and hence the arising structure is, strictly speaking, homoclinic. However, for the map $\boldsymbol{F^4}$ this intersection is formally heteroclinic, and the attractor on the Poincaré map (see Fig. 9a) is visually similar to the heteroclinic spiral attractor [45, 74], with the essential difference that it is discrete.

Remark. In order to show that the arising attractor is indeed a discrete spiral attractor, we have numerically found a value of the parameter E at which a heteroclinic structure connecting two fixed points P and C arises in the map $\boldsymbol{F^4}$. The search algorithm involved localizing the corresponding value of the energy parameter above and below by the deviation of the one-dimensional stable manifold of point C from the spiral along which it must converge (in backward time) on the two-dimensional unstable manifold of point P. In one case it deviated towards the center of the spiral, in the other case it deviated outside. After the required value had been localized, it was determined more precisely by the bisection method. Figure 8 shows the one-dimensional stable manifold of the fixed point C for the best estimate obtained for the value of the energy parameter, $E = E_{het} = 423.59597843$: the manifold lies visually in the two-dimensional unstable manifold of point P.

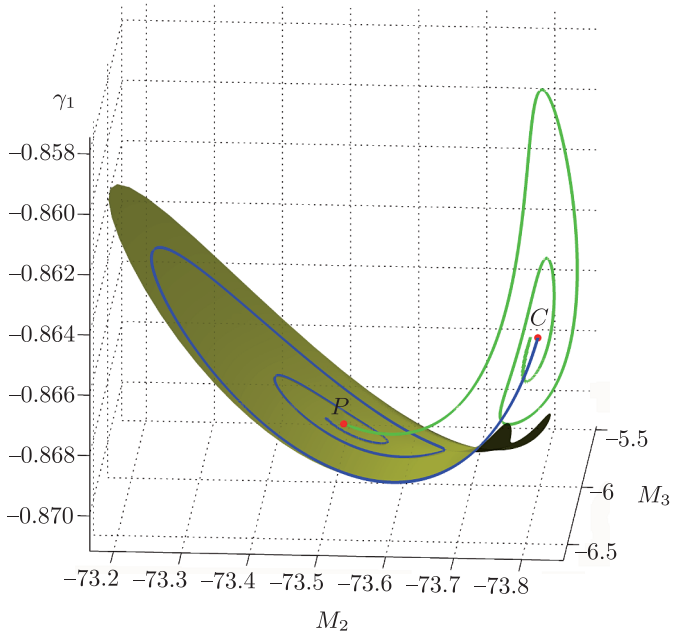

Fig. 8. At $E = E_{het} = 423.59597843$, the one-dimensional stable manifold of the fixed point C of the map $\boldsymbol{F^4}$ is visually superimposed onto the two-dimensional unstable manifold of point P.

We note that the behavior of the manifolds of the saddle-focus point 4SF of the map $\boldsymbol{F^4}$ in the case at hand is very similar to the behavior of separatrices in systems with continuous time when homoclinic bifurcations of equilibria arise. Figure 8 shows that the stable and the unstable manifold do not intersect, but coincide; moreover, there are no typical oscillations increasing as the manifolds approach the saddle-focus point.

We can offer the following explanation for this phenomenon. It turns out that the saddle-focus cycle of period 4 4SF arises quite nearby, as the energy decreases to $E = E_{PD} \approx 424.629$, from the saddle-focus cycle (1,2) of period 2 (2SF), which, after a period doubling bifurcation, is of type (2,1). Immediately after the bifurcation the multipliers of cycle 2SF are equal to $(1.0022, -0.9111, -0.9965)$, which is very close to the triplet $(1, -1, -1)$. As shown in [75, 76], the second iteration of the three-dimensional Poincaré map near such a point must be close to the map along the trajectory for some three-dimensional flow. That is, the map $\boldsymbol{F^4}$ in a neighborhood of the saddle-focus fixed point 4SF can indeed be well approximated by the three-dimensional flow.

Figure 9a shows a phase portrait of a heteroclinic discrete spiral attractor for $E = E_{het} = 423.59597843$ on the Poincaré map, where both elements of the cycle of period 4 are seen to belong to the attractor. Figure 9b shows the one-dimensional stable manifolds of points P and C, which form a heteroclinic structure.

The spectrum of Lyapunov exponents in the Poincaré section for a discrete spiral attractor is $(\Lambda_1 = 0.0194, \Lambda_2 = 0.0000, \Lambda_3 = -0.1116)$. In addition, an estimate of the correlation dimension of the attractor in the Poincaré section has been obtained: $D_{cor} = 2.10 \pm 0.03$, which agrees fairly well with the estimate of the Lyapunov dimension made by the Kaplan – Yorke formula: $D_{K-Y} = 2 + \Lambda_1/|\Lambda_3| \approx 2.17$.

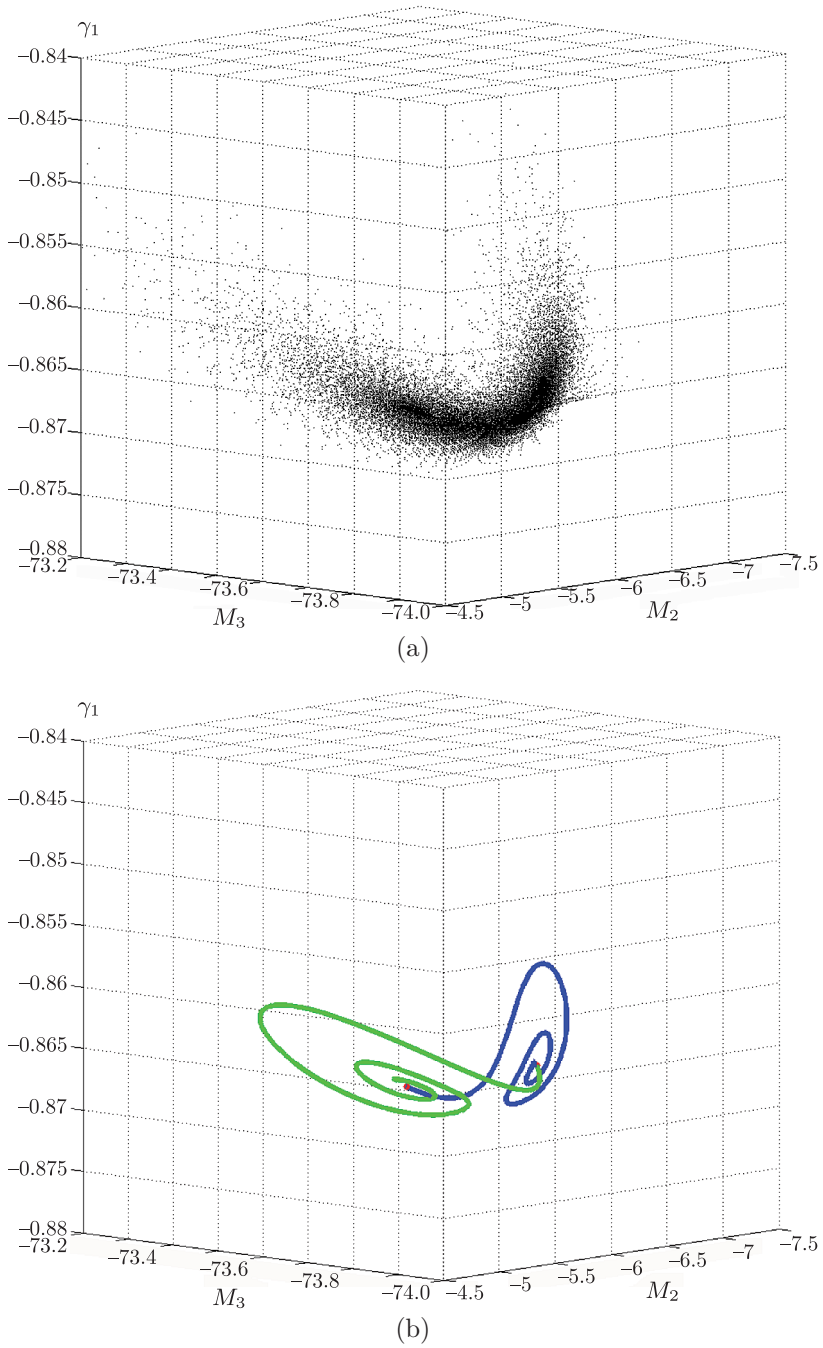

Fig. 9. (a) Phase portrait of a heteroclinic discrete spiral attractor and (b) arrangement of the one-dimensional stable manifolds of components P and C of the saddle-focus cycle of period 4 on the secant $M_1 = 0$ for $E = E_{het} = 423.59597843$.

5. ROLLING OF A CHAPLYGIN TOP IN ABSOLUTE SPACE

Let us examine the motion of a Chaplygin top, which corresponds to a discrete spiral attractor, in absolute space. For this, we supplement the system (2.1) with equations for the position of the center of mass and the orientation of the ball (2.2). Figure 10a shows the trajectory of the contact point of the Chaplygin top started from the saddle-focus point 4SF. Figures 10b show the trajectory of the contact point of the top for a heteroclinic discrete spiral attractor presented in Fig. 9a.

The behavior of the contact point of the top on the saddle-focus point 4SF is quasi-periodic. On the discrete spiral attractor, a chaotic component manifests itself in the behavior of the contact point; however, it is almost impossible to detect it visually. The contact point fills, as before, an

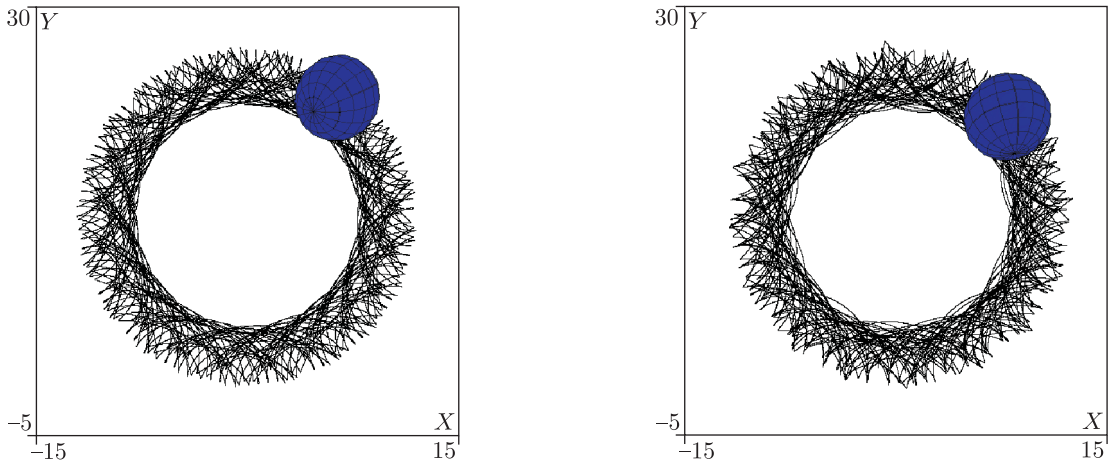

(a) $E = E_{het} = 423.59597843$ (b) $E = E_{het} = 423.59597843$

Fig. 10. Trajectory of the contact point of the Chaplygin top for different dynamical regimes: (a) the saddle-focus point 4SF from which a heteroclinic discrete spiral attractor has arisen, (b) the heteroclinic discrete spiral attractor shown in Fig. 9a.

annulus in the plane, and the appearance of the chaotic component cannot be detected by the harmonic analysis technique applied by the authors. The Fourier spectrum does not differ from the discrete one within the accuracy of calculations.

The trajectories of the point of contact shown in Fig. 10 have been calculated without taking into account the loss of contact of the body with the surface, which is highly probable when the center of mass is displaced. This is due to the fact that the loss of contact in such systems leads to paradoxical situations [80, 81] and requires a separate analysis.

6. CONCLUSION

To conclude, we present some considerations regarding the behavior of the contact point of the Chaplygin top, which are partially hypothetical in nature. In the case of zero displacement of the center of mass (the Chaplygin ball), the contact point undergoes a directed drift for almost all initial conditions, and its behavior is regular (for a proof, see [5]). In the case of displacement of the center of mass, but in the absence of a gravitational field, the trajectory of the contact point tends, as a rule, to quasi-periodic final motion, which is defined by simple attractors in the reduced phase space [13]. When a gravitational field is added, multistability breaks down and chaotic (including strange) attractors appear which occupy a much larger part of the phase space.

However, not for all complex attractors the trace of the contact point is distinctly chaotic in nature and admits diffusion or drift. Strange as it may seem, a substantial number of higher frequency harmonics are suppressed. As a result, the difference of the motion of the contact point from the quasi-periodic motion is insignificant and hence can hardly be detected in a natural experiment. In this sense, it would be interesting to explore other chaotic attractors which are typical of the system considered and can lead to a high degree of chaotization of the contact point. It is possible that the nonholonomic dissipation discussed in the introduction prohibits the realization of many attractors having strongly chaotic dynamics. In particular, the question remains open whether the system under study has hyperchaotic attractors (with two positive Lyapunov exponents) similar to those presented in [19] or [77–79]. As already noted in [2], it would be interesting to make a physical prototype of the ball which could exhibit the phenomena of reversal and strong chaotization of dynamics.

7. ACKNOWLEDGMENTS

The authors would like to extend particular gratitude to S. P. Kuznetsov, I. A. Bizyaev, S. V. Gonchenko and A. L. Shilnikov for useful discussions.

The work of A. V. Borisov (Introduction, Section 2 and Conclusion) was carried out within the framework of the state assignment for institutions of higher education and supported by the RFBR grant No. 15-08-09261-a. The work of A. O. Kazakov (Sections 1 and 5) was supported by the Basic Research Program at the National Research University Higher School of Economics (project 98), by the Dynasty Foundation, and by the RFBR grant No. 14-01-00344. The work of I. R. Sataev (Sections 3 and 4) was supported by the RSF grant No. 15-12-20035.

The computer simulation was carried out using the software package "Computer Dynamics: Chaos" (http://lab-en.ics.org.ru/lab/page/kompyuternaya-dinamika/).

REFERENCES

1. Shen, J., Schneider, D. A., and Bloch, A. M., Controllability and Motion Planning of a Multibody Chaplygin's Sphere and Chaplygin's Top, *Internat. J. Robust Nonlinear Control,* 2008, vol. 18, no. 9, pp. 905–945.
2. Borisov, A. V., Kazakov, A. O., and Sataev, I. R., The Reversal and Chaotic Attractor in the Nonholonomic Model of Chaplygin's Top, *Regul. Chaotic Dyn.,* 2014, vol. 19, no. 6, pp. 718–733.
3. Borisov, A. V., Mamaev, I. S., and Bizyaev, I. A., Historical and Critical Review of the Development of Nonholonomic Mechanics: The Classical Period, *Regul. Chaotic Dyn.,* 2016, vol. 21, no. 4, pp. 455–476.
4. Chaplygin, S. A., On a Ball's Rolling on a Horizontal Plane, *Regul. Chaotic Dyn.,* 2002, vol. 7, no. 2, pp. 131–148; see also: *Math. Sb.,* 1903, vol. 24, no. 1, pp. 139–168.
5. Borisov, A. V., Kilin, A. A., and Mamaev, I. S., The Problem of Drift and Recurrence for the Rolling Chaplygin Ball, *Regul. Chaotic Dyn.,* 2013, vol. 18, no. 6, pp. 832–859.
6. Sataev, I. R. and Kazakov, A. O., Scenarios of Transition to Chaos in the Nonholonomic Model of a Chaplygin Top, *Nelin. Dinam.,* 2016, vol. 12, no. 2, pp. 235–250 (Russian).
7. Borisov, A. V. and Mamaev, I. S., Strange Attractors in Rattleback Dynamics, *Physics–Uspekhi,* 2003, vol. 46, no. 4, pp. 393–403; see also: *Uspekhi Fiz. Nauk,* 2003, vol. 173, no. 4, pp. 407–418.
8. Borisov, A. V., Jalnine, A. Yu., Kuznetsov, S. P., Sataev, I. R., and Sedova, J. V., Dynamical Phenomena Occurring due to Phase Volume Compression in Nonholonomic Model of the Rattleback, *Regul. Chaotic Dyn.,* 2012, vol. 17, no. 6, pp. 512–532.
9. Gonchenko, A. S., Gonchenko, S. V., and Kazakov, A. O., Richness of Chaotic Dynamics in Nonholonomic Models of a Celtic Stone, *Regul. Chaotic Dyn.,* 2013, vol. 18, no. 5, pp. 521–538.
10. Kozlov, V. V., On the Integration Theory of Equations of Nonholonomic Mechanics, *Regul. Chaotic Dyn.,* 2002, vol. 7, no. 2, pp. 161–176.
11. Borisov, A. V., Mamaev, I. S., and Bizyaev, I. A., The Jacobi Integral in Nonholonomic Mechanics, *Regul. Chaotic Dyn.,* 2015, vol. 20, no. 3, pp. 383–400.
12. Fassò, F. and Sansonetto, N., Conservation of Energy and Momenta in Nonholonomic Systems with Affine Constraints, *Regul. Chaotic Dyn.,* 2015, vol. 20, no. 4, pp. 449–462.
13. Borisov, A. V. and Mamaev, I. S., The Rolling Motion of a Rigid Body on a Plane and a Sphere: Hierarchy of Dynamics, *Regul. Chaotic Dyn.,* 2002, vol. 7, no. 2, pp. 177–200.
14. Vitolo, R., Broer, H., and Simó, C., Quasi-Periodic Bifurcations of Invariant Circles in Low-Dimensional Dissipative Dynamical Systems, *Regul. Chaotic Dyn.,* 2011, vol. 16, nos. 1–2, pp. 154–184.
15. Wilczak, D., Serrano, S., and Barrio, R., Coexistence and Dynamical Connections between Hyperchaos and Chaos in the 4D Rössler System: A Computer-Assisted Proof, *SIAM J. Appl. Dyn. Syst.,* 2016, vol. 15, no. 1, pp. 356–390.
16. Barrio, R., Martínez, M. A., Serrano, S., and Wilczak, D., When Chaos Meets Hyperchaos: 4D Rössler Model, *Phys. Lett. A,* 2015, vol. 379, no. 38, pp. 2300–2305.
17. Li, Ch. and Sprott, J. C., Coexisting Hidden Attractors in a 4-D Simplified Lorenz System, *Internat. J. Bifur. Chaos Appl. Sci. Engrg.,* 2014, vol. 24, no. 3, 1450034, 12 pp.
18. Rössler, O. E., Continuous Chaos: Four Prototype Equations, *Ann. New York Acad. Sci.,* 1979, vol. 316, no. 1, pp. 376–392.
19. Rössler, O. E., An Equation for Hyperchaos, *Phys. Lett. A,* 1979, vol. 71, no. 2, pp. 155–157.
20. Gonchenko, A. S. and Gonchenko, S. V., Variety of Strange Pseudohyperbolic Attractors in Three-Dimensional Generalized Hénon Maps, *Phys. D,* 2016, vol. 337, pp. 43–57.
21. Dullin, H. R. and Meiss, J. D., Quadratic Volume-Preserving Maps: Invariant Circles and Bifurcations, *SIAM J. Appl. Dyn. Syst.,* 2009, vol. 8, no. 1, pp. 76–128.
22. Mireles James, J. D., Quadratic Volume-Preserving Maps: (Un)stable Manifolds, Hyperbolic Dynamics, and Vortex-Bubble Bifurcations, *J. Nonlinear Sci.,* 2013, vol. 23, no. 4, pp. 585–615.
23. Borisov, A. V., Mamaev, I. S., and Kilin, A. A., Rolling of a Ball on a Surface: New Integrals and Hierarchy of Dynamics, *Regul. Chaotic Dyn.,* 2002, vol. 7, no. 2, pp. 201–219.
24. Borisov, A. V., Mamaev, I. S., and Kilin, A. A., Stability of Steady Rotations in the Nonholonomic Routh Problem, *Regul. Chaotic Dyn.,* 2008, vol. 13, no. 4, pp. 239–249.

25. Borisov, A. V., Mamaev, I. S., and Bizyaev, I. A., The Hierarchy of Dynamics of a Rigid Body Rolling without Slipping and Spinning on a Plane and a Sphere, *Regul. Chaotic Dyn.,* 2013, vol. 18, no. 3, pp. 277–328.
26. Borisov, A. V., Kazakov, A. O., and Kuznetsov, S. P., Nonlinear Dynamics of the Rattleback: A Nonholonomic Model, *Physics–Uspekhi,* 2014, vol. 57, no. 5, pp. 453–460; see also: *Uspekhi Fiz. Nauk,* 2014, vol. 184, no. 5, pp. 493–500.
27. Bizyaev, I. A., Borisov, A. V., and Kazakov, A. O., Dynamics of the Suslov Problem in a Gravitational Field: Reversal and Strange Attractors, *Regul. Chaotic Dyn.,* 2015, vol. 20, no. 5, pp. 605–626.
28. Gonchenko, A. S., Gonchenko, S. V., and Shilnikov, L. P., Towards Scenarios of Chaos Appearance in Three-Dimensional Maps, *Nelin. Dinam.,* 2012, vol. 8, no. 1, pp. 3–28 (Russian).
29. Borisov, A. V., Kazakov, A. O., and Pivovarova, E. N., Regular and Chaotic Dynamics in the Rubber Model of a Chaplygin Top, *Regul. Chaotic Dyn.,* 2016, vol. 21, no. 7, pp. 885–901.
30. Borisov, A. V. and Kuznetsov, S. P., Regular and Chaotic Motions of a Chaplygin Sleigh under Periodic Pulsed Torque Impacts, *Regul. Chaotic Dyn.,* 2016, vol. 21, no. 7, pp. 792–803.
31. Borisov, A. V., Kilin, A. A., and Mamaev, I. S., How to Control Chaplygin's Sphere Using Rotors, *Regul. Chaotic Dyn.,* 2012, vol. 17, nos. 3–4, pp. 258–272.
32. Borisov, A. V., Kilin, A. A., and Mamaev, I. S., How to Control Chaplygin's Sphere Using Rotors: 2, *Regul. Chaotic Dyn.,* 2013, vol. 18, nos. 1–2, pp. 144–158.
33. Tafrishi, S. A., Veres, S. M., Esmaeilzadeh, E., and Svinin, M., Dynamical Behavior Investigation and Analysis of Novel Mechanism for Simulated Spherical Robot named "RollRoller", arXiv:1610.06218 (2016).
34. Ott, E., Grebogi, C., and Yorke, J. A., Controlling Chaos, *Phys. Rev. Lett.,* 1990, vol. 64, no. 11, pp. 1196–1199.
35. Borisov, A. V., Kazakov, A. O., and Kuznetsov, S. P., Nonlinear Dynamics of the Rattleback: A Nonholonomic Model, *Physics–Uspekhi,* 2014, vol. 57, no. 5, pp. 453–460; see also: *Uspekhi Fiz. Nauk,* 2014, vol. 184, no. 5, pp. 493–500.
36. Borisov, A. V. and Fedorov, Yu. N., On Two Modified Integrable Problems in Dynamics, *Mosc. Univ. Mech. Bull.,* 1995, vol. 50, no. 6, pp. 16–18; see also: *Vestnik Moskov. Univ. Ser. 1. Mat. Mekh.,* 1995, no. 6, pp. 102–105.
37. Borisov, A. V., Fedorov, Yu. N., and Mamaev, I. S., Chaplygin Ball over a Fixed Sphere: An Explicit Integration, *Regul. Chaotic Dyn.,* 2008, vol. 13, no. 6, pp. 557–571.
38. Borisov, A. V. and Mamaev, I. S., Topological Analysis of an Integrable System Related to the Rolling of a Ball on a Sphere, *Regul. Chaotic Dyn.,* 2013, vol. 18, no. 4, pp. 356–371.
39. Shil'nikov, L. P., A Case of the Existence of a Countable Number of Periodic Motions, *Soviet Math. Dokl.,* 1965, vol. 6, pp. 163–166; see also: *Dokl. Akad. Nauk SSSR,* 1965, vol. 169, no. 3, pp. 558–561.
40. Rössler, O. E., An Equation for Continuous Chaos, *Phys. Lett. A,* 1976, vol. 57, no. 5, pp. 397–398.
41. Arnéodo, A., Coullet, P., and Tresser, C., Oscillators with Chaotic Behavior: An Illustration of a Theorem by Shil'nikov, *J. Statist. Phys.,* 1982, vol. 27, no. 1, pp. 171–182.
42. Arnéodo, A., Coullet, P., and Tresser, C., Occurence of Strange Attractors in Three-Dimensional Volterra Equations, *Phys. Lett. A,* 1980, vol. 79, no. 4, pp. 259–263.
43. Arnéodo, A., Coullet, P., and Tresser, C., Possible New Strange Attractors with Spiral Structure, *Comm. Math. Phys.,* 1981, vol. 79, no. 4, pp. 573–579.
44. Belykh, V. N. and Nekorkin, V. I., Qualitative Investigation of a System of Three Differential Equations in the Theory of Phase Synchronization, *J. Appl. Math. Mech.,* 1975, vol. 39, no. 4, pp. 615–622; see also: *Prikl. Mat. Mekh.,* 1975, vol. 39, no. 4, pp. 642–469.
45. Chua, L. O., Komuro, M., and Matsumoto, T., The Double Scroll Family: 1. Rigorous Proof of Chaos, *IEEE Trans. Circuits and Systems,* 1986, vol. 33, no. 11, pp. 1072–1097;
Chua, L. O., Komuro, M., and Matsumoto, T., The Double Scroll Family: 2. Rigorous Analysis of Bifurcation Phenomena, 1986, vol. 33, no. 11, pp. 1097–1118.
46. Anishchenko, V. S., *Complicated Oscillations in Simple Systems,* Moscow: Nauka, 1990 (Russian).
47. Arecchi, F. T., Meucci, R., and Gadomski, W., Laser Dynamics with Competing Instabilities, *Phys. Rev. Lett.,* 1987, vol. 58, no. 21, pp. 2205–2208.
48. Arecchi, F. T., Lapucci, A., Meucci, R., Roversi, J. A., and Coullet, P. H., Experimental Characterization of Shil'nikov Chaos by Statistics of Return Times, *Europhys. Lett.,* 1988, vol. 6, no. 8, pp. 677–682.
49. Pisarchik, A. N., Meucci, R., and Arecchi, F. T., Theoretical and Experimental Study of Discrete Behavior of Shilnikov Chaos in a CO_2 Laser, *Eur. Phys. J. D,* 2001, vol. 13, no. 3, pp. 385–391.
50. Zhou, C. S., Kurths, J., Allaria, E., Boccaletti, S., Meucci, R., and Arecchi, F. T., Constructive Effects of Noise in Homoclinic Chaotic Systems, *Phys. Rev. E,* 2003, vol. 67, no. 6, 066220, 9 pp.
51. Argoul, F., Arnéodo, A., and Richetti, P., Experimental Evidence for Homoclinic Chaos in the Belousov – Zhabotinskii Reaction, *Phys. Lett. A,* 1987, vol. 120, no. 6, pp. 269–275.
52. Arnéodo, A., Argoul, F., Elezgaray, J., and Richetti, P., Homoclinic Chaos in Chemical Systems, *Phys. D,* 1993, vol. 62, nos. 1–4, pp. 134–169.
53. Braun, Th., Lisboa, J. A., and Gallas, J. A. C., Evidence of Homoclinic Chaos in the Plasma of a Glow Discharge, *Phys. Rev. Lett.,* 1992, vol. 68, no. 18, pp. 2770–2773.

54. Feudel, U., Neiman, A., Pei, X., Wojtenek, W., Braun, H., Huber, M., and Moss, F., Homoclinic Bifurcation in a Hodgkin – Huxley Model of Thermally Sensitive Neurons, *Chaos,* 2000, vol. 10, no. 1, pp. 231–239.
55. Parthimos, D., Edwards, D. H., and Griffith, T. M., Shil'nikov Homoclinic Chaos Is Intimately Related to Type-III Intermittency in Isolated Rabbit Arteries: Role of Nitric Oxide, *Phys. Rev. E,* 2003, vol. 67, no. 5, 051922, 7 pp.
56. Koper, M. T. M., Gaspard, P., and Sluyters, J. H., Mixed-Mode Oscillations and Incomplete Homoclinic Scenarios to a Saddle Focus in the Indium/Thiocyanate Electrochemical Oscillator, *J. Chem. Phys.,* 1992, vol. 97, no. 11, pp. 8250–8260.
57. Chedjou, J. C., Woafo, P., and Domngang, S., Shilnikov Chaos and Dynamics of a Self-Sustained Electromechanical Transducer, *J. Vib. Acoust.,* 2001, vol. 123, no. 2, pp. 170–174.
58. Bassett, M. R. and Hudson, J. L., Shil'nikov Chaos during Copper Electrodissolution, *J. Phys. Chem.,* 1988, vol. 92, no. 24, pp. 6963–6966.
59. Noh, T., Shil'nikov Chaos in the Oxidation of Formic Acid with Bismuth Ion on Pt Ring Electrode, *Electrochim. Acta,* 2009, vol. 54, no. 13, pp. 3657–3661.
60. Rucklidge, A. M., Chaos in a Low-Order Model of Magnetoconvection, *Phys. D,* 1993, vol. 62, nos. 1–4, pp. 323–337.
61. Henderson, M. E., Levi, M., and Odeh, F., The Geometry and Computation of the Dynamics of Coupled Pendula, *Internat. J. Bifur. Chaos Appl. Sci. Engrg.,* 1991, vol. 1, no. 1, pp. 27–50.
62. Smale, S., Diffeomorphisms with Many Periodic Points, in *Differential and Combinatorial Topology: A Symposium in Honor of Marston Morse,* S. S. Cairns (Ed.), Princeton, N.J.: Princeton Univ. Press, 1965, pp. 63–80.
63. Shilnikov, L. P., On a Poincaré – Birkhoff Problem, *Math. USSR-Sb.,* 1967, vol. 3, no. 3, pp. 353–371; see also: *Mat. Sb. (N. S.),* 1967, vol. 74(116), no. 3, pp. 378–397.
64. Rössler, O. E., Different Types of Chaos in Two Simple Differential Equations, *Z. Naturforsch. A,* 1976, vol. 31, no. 12, pp. 1664–1670.
65. Letellier, C., Dutertre, P., and Maheu, B., Unstable Periodic Orbits and Templates of the Rössler System: Toward a Systematic Topological Characterization, *Chaos,* 1995, vol. 5, no. 1, pp. 271–282.
66. Barrio, R., Blesa, F., Serrano, S., and Shilnikov, A., Global Organization of Spiral Structures in Bi-parameter Space of Dissipative Systems with Shilnikov Saddle-Foci, *Phys. Rev. E,* 2011, vol. 84, no. 3, 035201, 5 pp.
67. Broer, H., Simó, C., and Vitolo, R., Bifurcations and Strange Attractors in the Lorenz-84 Climate Model with Seasonal Forcing, *Nonlinearity,* 2002, vol. 15, no. 4, pp. 1205–1267.
68. Borisov, A. V. and Mamaev, I. S., *Dynamics of a Rigid Body: Hamiltonian Methods, Integrability, Chaos,* 2nd ed., Izhevsk: R&C Dynamics, Institute of Computer Science, 2005 (Russian).
69. Kuznetsov, S. P., Effect of a Periodic External Perturbation on a System Which Exhibits an Order-Chaos Transition through Period-Doubling-Bifurcations Metal-Insulator-Semiconductor, *JETP Lett.,* 1984, vol. 39, no. 3, pp. 133–136; see also: *Pis'ma v Zh. Èksper. Teoret. Fiz.,* 1984, vol. 39, no. 3, pp. 113–116.
70. Anishchenko V. S. *Stochastic oscillations in radiophysical systems: P. 2,* Saratov: Saratov Gos. Univ., 1986 (Russian).
71. Arnéodo, A., Coullet, P. H., and Spiegel, E. A., Cascade of Period Doublings of Tori, *Phys. Lett. A,* 1983, vol. 94, no. 1, pp. 1–6.
72. Kaneko, K., Doubling of Torus, *Progr. Theoret. Phys.,* 1983, vol. 69, no. 6, pp. 1806–1810.
73. Krauskopf, B. and Osinga, H., Growing 1D and Quasi-2D Unstable Manifolds of Maps, *J. Comput. Phys.,* 1998, vol. 146, no. 1, pp. 404–419.
74. Shilnikov, L. P., Chua's Circuit: Rigorous Results and Future Problems, *Internat. J. Bifur. Chaos Appl. Sci. Engrg.,* 1994, vol. 4, no. 03, pp. 489–519.
75. Shil'nikov, A. L., Shil'nikov, L. P., and Turaev, D. V., Normal Forms and Lorenz Attractors, *Internat. J. Bifur. Chaos Appl. Sci. Engrg.,* 1993, vol. 3, no. 5, pp. 1123–1139.
76. Gonchenko, S. V., Ovsyannikov, I. I., Simó, C., and Turaev, D., Three-Dimensional Hénon-Like Maps and Wild Lorenz-Like Attractors, *Internat. J. Bifur. Chaos Appl. Sci. Engrg.,* 2005, vol. 15, no. 11, pp. 3493–3508.
77. Baier, G. and Klein, M., Maximum Hyperchaos in Generalized Hénon Maps, *Phys. Lett. A,* 1990, vol. 151, nos. 6–7, pp. 281–284.
78. Kapitaniak, T., Thylwe, K.-E., Cohen, I., and Wojewoda, J., Chaos-Hyperchaos Transition, *Chaos Solitons Fractals,* 1995, vol. 5, no. 10, pp. 2003–2011.
79. Stefański, K., Modelling Chaos and Hyperchaos with 3-D Maps, *Chaos Solitons Fractals,* 1998, vol. 9, nos. 1–2, pp. 83–93.
80. Ivanov, A. P., On Detachment Conditions in the Problem on the Motion of a Rigid Body on a Rough Plane, *Regul. Chaotic Dyn.,* 2008, vol. 13, no. 4, pp. 355–368.
81. Ivanov, A. P., Geometric Representation of Detachment Conditions in Systems with Unilateral Constraints, *Regul. Chaotic Dyn.,* 2008, vol. 13, no. 5, pp. 435–442.